



Communication

Lophatherum gracile Bronghiart Suppresses Receptor Activator of Nuclear Factor Kappa-B Ligand-Stimulated Osteoclastogenesis and Prevents Ovariectomy-Induced Osteoporosis

Sung-Ju Lee ^{1,†}, Seon-A Jang ^{2,†}, Seong Cheol Kim ¹, Jin Ah Ryuk ¹ and Hyunil Ha ^{1,*}

¹ KM Convergence Research Division, Korea Institute of Oriental Medicine, Yuseong-daero 1672, Daejeon 34054, Republic of Korea

² Future Technology Research Center, KT&G Corporation, 30, Gajeong-ro, Yuseong-gu, Daejeon 34128, Republic of Korea

* Correspondence: hyunil74@kiom.re.kr; Tel.: +82-42-868-9367

† These authors contributed equally to this work.

Abstract: *Lophatherum gracile* Bronghiart, used in traditional herbal medicine, has many biological properties including antiviral, antipyretic, antitumor, vasorelaxation, and neutrophilic inflammatory effects. However, its modulatory effects on bone metabolism have not been investigated previously. In this study, we examined the effects of a water extract of the leaves of *L. gracile* (WELG) on osteoclast differentiation and bone loss, and explored its underlying mechanisms. We found that WELG inhibits osteoclastogenesis by suppressing both receptor activator of nuclear factor- κ B ligand (RANKL)-induced early activation of mitogen-activated protein kinases (MAPKs) and nuclear factor- κ B (NF- κ B)- and RANKL-induced modulation of the positive and negative regulators of osteoclastogenesis in osteoclast precursors. In vivo study demonstrated that WELG protects against bone loss, weight gain, and fat accumulation without affecting uterine atrophy in an ovariectomy-induced postmenopausal osteoporosis mice model. In addition, photochemical analysis of WELG identified active constituents known to have bone-protective effects. Overall, the results of this study suggest that WELG can be a potential candidate for therapy and prevention of postmenopausal osteoporosis.

Keywords: *Lophatherum gracile* Bronghiart; osteoporosis; bone loss; ovariectomy



Citation: Lee, S.-J.; Jang, S.-A.; Kim, S.C.; Ryuk, J.A.; Ha, H. *Lophatherum gracile* Bronghiart Suppresses Receptor Activator of Nuclear Factor Kappa-B Ligand-Stimulated Osteoclastogenesis and Prevents Ovariectomy-Induced Osteoporosis. *Int. J. Mol. Sci.* **2022**, *23*, 13942. <https://doi.org/10.3390/ijms232213942>

Academic Editor: Chih-Hsin Tang

Received: 16 October 2022

Accepted: 10 November 2022

Published: 11 November 2022

Publisher's Note: MDPI stays neutral with regard to jurisdictional claims in published maps and institutional affiliations.



Copyright: © 2022 by the authors. Licensee MDPI, Basel, Switzerland. This article is an open access article distributed under the terms and conditions of the Creative Commons Attribution (CC BY) license (<https://creativecommons.org/licenses/by/4.0/>).

1. Introduction

Bone homeostasis is regulated by osteoclast-induced bone resorption and bone formation mediated by osteoblasts, which is a reconstituted step of bone tissue renewal for maintaining bone homeostasis in normal adult bones [1]. However, excessive osteoclast differentiation and activation can cause osteoporosis due to an imbalance between bone resorption and formation [2,3]. Osteoporosis is a metabolic bone disease characterized by extremely low bone density occurring mainly in the elderly, especially in menopausal women [2,3]. Additionally, this disease can cause bone fracture symptoms owing to enhanced bone brittleness and thinning through ultrastructural disruption [4]. Osteoclasts are giant multinucleated cells that have undergone differentiation and fusion of macrophages and monocyte-descended precursor cells and activation [5,6]. Osteoclast differentiation is initiated by receptor activator of nuclear factor- κ B ligand (RANKL) and macrophage-colony-stimulating factor (M-CSF), which are engaged by various cells, including stromal cells, osteoblasts, and osteocytes [5,6]. After RANKL binds to the receptor RANK on osteoclast precursors, RANK recruits TNF-receptor-associated factors (TRAFs) [5,6]. The combined RANKL/RANK/TRAFs axis activates nuclear factor- κ B (NF- κ B) and mitogen-activated protein kinase (MAPK) signaling pathways, which upregulates several downstream transcription factors, including nuclear factor of activated T cells c1 (NFATc1) and

cellular oncogene fos (c-Fos) [7–11]. Moreover, NFATc1 functions as a master transcription factor and upregulates the expression of specific osteoclastogenesis-associated genes such as tartrate-resistant acid phosphatase (TRAP), cathepsin K (Ctsk), dendritic cell-specific transmembrane proteins (DC-STAMP), and ATPase H⁺ transporting V0 subunit D2 (Atp6v0d2) [12,13]. Targeted regulation of these signaling pathways can prevent or treat bone loss caused by excessive osteoclast differentiation and activation [14].

Lophatherum gracile Bronghiart (*L. gracile*) is affiliated with the family Gramineae and is generally found in southern China. The leaves of *L. gracile* were widely used in traditional herbal medicine from old times, mostly, to treat inflammation and fever. Recently, a diversity of biological and pharmacological research on *L. gracile* has been conducted regarding topics such as its anti-viral activity, anti-cancer, fever reduction, vasorelaxation protection, and neutrophilic inflammation effects, and prevention of hyperglycemia [15–18]. In addition, several flavonoids purified from ethanolic extracts of the leaves of *L. gracile* show potent antioxidant and hepatoprotective effects [19]. However, the effects of *L. gracile* on bone metabolism have not yet been reported.

In this study, we studied the inhibitory effects of a water extract of the leaves of *L. gracile* (WELG) on osteoclastogenesis and demonstrated its fundamental mechanisms. We also examined its beneficial effects against bone loss in an ovariectomy (OVX)-induced postmenopausal osteoporosis mouse model. Our findings provide evidence for the beneficial effects of WELG on osteoclast-associated osteoporosis.

2. Results and Discussion

2.1. Suppression Effect of WELG on Osteoclast Differentiation

Osteocytes regulate osteoclast differentiation and bone resorption through the secreted essential pro-osteoclastogenic molecule, RANKL, and its inhibitor, osteoprotegerin (OPG) [20,21]. To assess the role of WELG in osteoclastogenesis, MLO-Y4, osteocyte-like cells [22], co-cultured with bone marrow derived macrophages (BMMs) were treated with various concentrations of WELG. Stimulation of the co-culture with 1 α , 25-dihydroxyvitamin D3 (VitD3) increased osteoclast formation. However, treatment with WELG significantly and dose-dependently inhibited osteoclast formation in the co-culture system (Figure 1A,B). VitD3 stimulated the mRNA expression of tumor necrosis factor ligand superfamily member 11 (Tnfsf11) gene encoding RANKL and decreased the mRNA expression of tumor necrosis factor receptor superfamily member 11B (Tnfrsf11b) gene encoding OPG in MLO-Y4 cells, which was not affected by WELG (Figure 1C). Thus, we speculated that WELG might directly inhibit osteoclast differentiation independently of its action on MLO-Y4 cells to support osteoclast differentiation. To assess the direct inhibitory effect of WELG on osteoclastogenesis, osteoclast precursors, BMMs, were stimulated with RANKL to induce osteoclast differentiation. WELG suppressed RANKL-induced formation of TRAP-positive multinucleated osteoclasts in a dose-dependent manner (Figure 2A,B). Treatments of BMMs with WELG at doses showing inhibitory effects on osteoclast differentiation did not decrease but slightly increased cell viability, assessed by a Cell Counting Kit-8 (CCK-8) assay (Figure 2C). These results demonstrated that WELG directly inhibits osteoclast differentiation processes triggered by RANKL in osteoclast precursor cells.

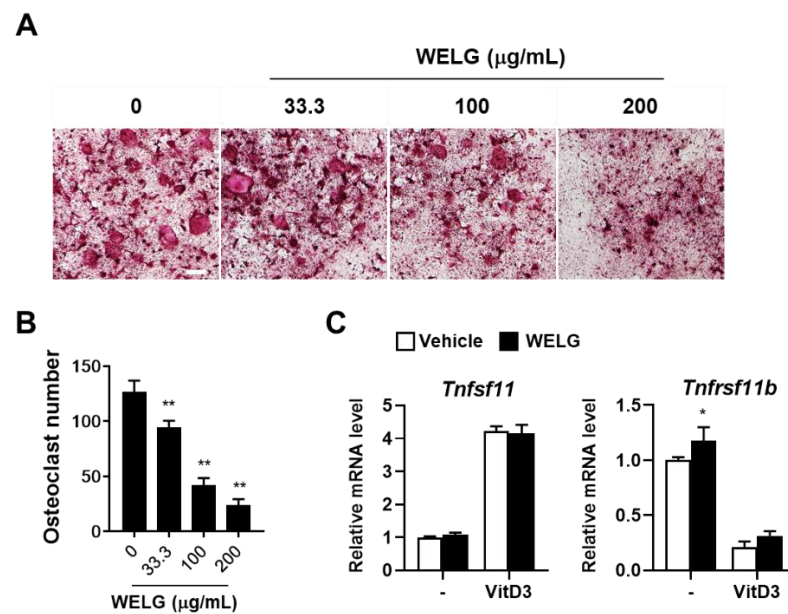


Figure 1. Suppression effect of WELG on osteoclast formation in co-cultures of osteocytes and osteoclast precursors. The co-cultures of MLO-Y4 and BMMs were treated with or without WELG for 5 days in the presence of VitD3 (10 nM). (A) Representative TRAP-staining images of the co-cultures (scale bar, 100 μm). (B) The number of osteoclasts, TRAP-stained multinucleated cells including more than three nuclei. (C) MLO-Y4 cells were treated with or without WELG (200 μg/mL) and VitD3 (10 nM) for 1 day. *Tnfsf11* and *Tnfrsf11b* mRNA expression levels were quantified by quantitative real-time polymerase chain reaction. * $p < 0.05$, ** $p < 0.01$ versus vehicle.

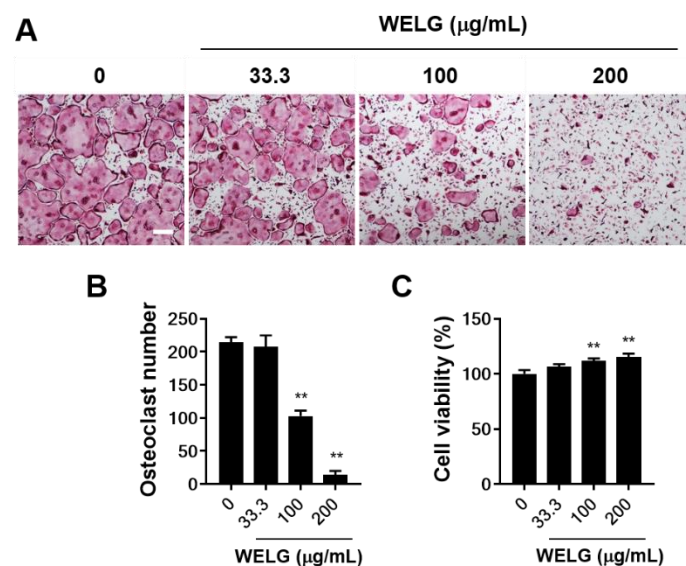


Figure 2. Suppression effect of WELG on RANKL-stimulated osteoclastogenesis. BMMs were treated with or without WELG in the presence of M-CSF (60 ng/mL) and RANKL (50 ng/mL) for 4 days. (A) TRAP-staining images of the cultures (scale bar, 100 μm). (B) The number of osteoclasts generated in the cultures. (C) Cell viability of BMMs after 24 h of treatment with WELG. ** $p < 0.01$ versus vehicle.

2.2. Suppression Effect of WELG on RANKL Signaling Pathways during Osteoclast Differentiation

RANKL-mediated signaling cascades play a key role in controlling osteoclastogenesis. RANKL binds with RANK and activates the MAPK and NF-κB pathways via TRAF adaptor proteins, which leads to upregulation of c-Fos and NFATc1 [7–11]. NFATc1 and

c-Fos are the main transcription factors for osteoclast formation as well as differentiation and upregulation of osteoclast-specific genes, including TRAP, matrix metalloproteinase 9 (Mmp9), integrin beta 3 (Itgb3), and Ctsk [13,23]. To explore the inhibitory mechanism of WELG on osteoclast differentiation, we examined the effects of WELG on RANKL-induced expression and activation of these molecules. Treatment of BMMs with RANKL increased NFATc1 mRNA and protein expression, which was significantly inhibited by WELG (Figure 3A,B). Subsequently, WELG suppressed RANKL-induced upregulation of osteoclastic marker genes Ctsk, Itgb3, and Mmp9 (Figure 3B). Interferon regulatory factor 8 (IRF8) and v-maf avian musculoaponeurotic fibrosarcoma oncogene homolog B (MafB), known as the negative osteoclast transcription factors, suppress the transcriptional activity of NFATc1 [24,25]. These negative osteoclast transcription factors are negatively controlled by transcriptional repressors such as positive regulatory domain zinc finger protein 1 (Prdm1; encoding Blimp1) [26]. WELG significantly suppressed a RANKL-induced decrease in *Irf8* and *MarB* expression and increase in *Prdm1* expression (Figure 3B). RANKL-induced protein, but not mRNA, expression of c-Fos, an upstream transcription factor of NFATc1 for osteoclastogenesis [23], was also inhibited by WELG (Figure 3A,B). Because interferon- β (IFN- β) has been shown to inhibit RANKL-induced protein, but not mRNA, expression of c-Fos [27], we investigated the effect of WELG on *Ifnb1* expression. Although WELG suppressed *Ifnb1* expression in the absence of RANKL, it inhibited the decrease in *Ifnb1* expression induced by RANKL (Figure 3B), suggesting that this may contribute, in part, to the reduction of c-Fos protein levels by WELG. Taken together, these results suggest that WELG inhibits osteoclast differentiation by suppressing both upregulation of the positive transcription factors and downregulation of the negative transcription factors of osteoclastogenesis.

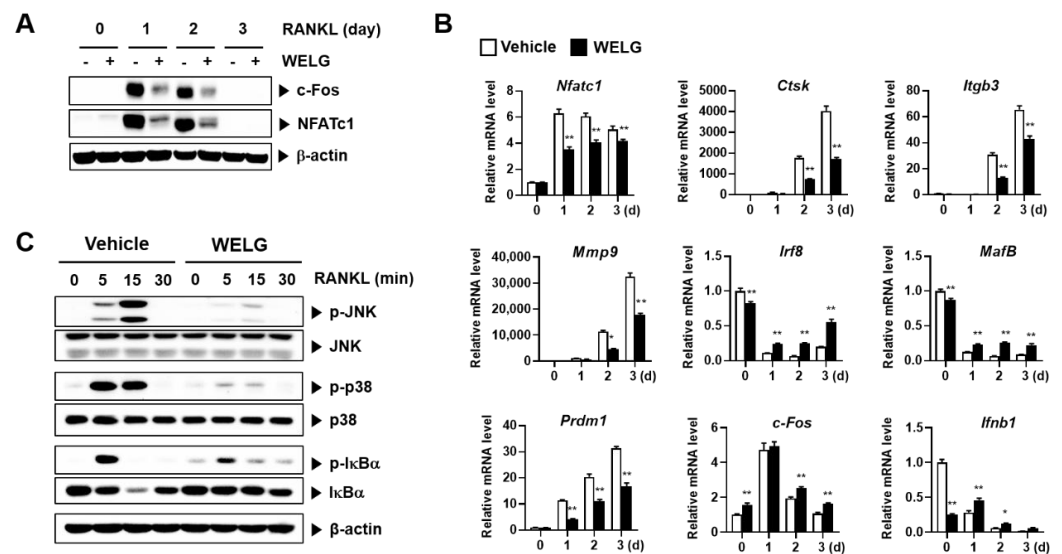


Figure 3. Suppression effect of WELG on RANKL-stimulated signal pathways in osteoclastogenesis. BMMs were activated by RANKL (50 ng/mL) treatment for the indicated days following pretreatment with vehicle or WELG (200 μ g/mL) for 3 h. (A) The levels of c-Fos and NFATc1 protein on the indicated days were analyzed by Western blotting. (B) The levels of mRNA genes involved in osteoclastogenesis were analyzed by quantitative real-time polymerase chain reaction. * $p < 0.05$, ** $p < 0.01$ versus vehicle. (C) BMMs were activated by RANKL (50 ng/mL) for the indicated times following pretreatment with vehicle or WELG (200 μ g/mL) for 3 h. The proteins related to RANKL-induced NF- κ B and MAPK signaling pathways were analyzed by Western blotting. All tests were repeated at least three times.

NF- κ B and MAPK (c-Jun N-terminal protein kinase (JNK) and p38 subfamilies) pathways are regarded as the main early signaling events activated during osteoclast differentiation through the involvement of c-Fos and NFATc1 induction [9–11]. To further elucidate

the inhibitory mechanisms of WELG on osteoclastogenesis, we examined the effects of WELG on RANKL-stimulated MAPKs and NF- κ B pathways in BMMs. As shown in Figure 3C, treatment of BMMs with WELG blunted RANKL-induced phosphorylation of JNK and p38 MAPKs. WELG also inhibited RANKL-induced activation of the classical NF- κ B pathway, as determined by I κ B α phosphorylation and degradation. Thus, these results suggest that the inhibition of WELG on RANKL-induced early signaling events including MAPK and NF- κ B pathways may account for its modulatory effects on the expression of the positive and negative osteoclastogenic transcription factors.

2.3. Protective Effects of WELG on OVX-Induced Bone Loss and Fat Accumulation

In postmenopausal osteoporosis, due to estrogen deficiency, increasing osteoclast formation and activation leads to bone loss [4]. Having confirmed that WELG inhibited RANKL-stimulated osteoclast formation, we investigated the effects of WELG on OVX-induced osteoporosis in vivo. Mice were orally administered WELG for 6 weeks beginning at 1 week after OVX surgery. Three-dimensional images of the distal femur by micro-computed tomography showed that metaphyseal trabecular bone loss was strongly induced in OVX mice compared to that in sham mice. In contrast, trabecular bone loss was recovered by oral administration of WELG at low and high doses (Figure 4A). Quantitative analysis confirmed that trabecular bone mineral density (BMD), bone volume/tissue volume (BV/TV), trabecular thickness (Tb.Th), and trabecular number (Tb.N) in the OVX group were highly decreased compared to those in the sham group. In contrast, trabecular separation (Tb.Sp) in the OVX group was significantly higher than that in the sham group. WELG administration significantly reversed OVX-induced changes in the trabecular bone structural parameters BMD, BV/TV, Tb.N, Tb.Th, and Tb.Sp (Figure 4B). To investigate the mechanisms underlying the inhibitory effects of WELG on bone loss, we measured serum concentrations of C-terminal cross-linked telopeptides of type I collagen (CTX, a bone resorption marker), TRAP 5b as a marker of osteoclast number, and procollagen type I N-terminal propeptide (PINP, a bone resorption marker). Serum CTX levels tended to decrease in the WELG groups compared to those in the OVX group. Similarly, TRAP 5b levels were also reduced in the WELG groups. In contrast, WELG administration did not affect PINP levels decreased by OVX (Figure 4C). Thus, it is likely that the anti-osteoclastic action of WELG might mainly contribute to its protective effect on OVX-induced bone loss.

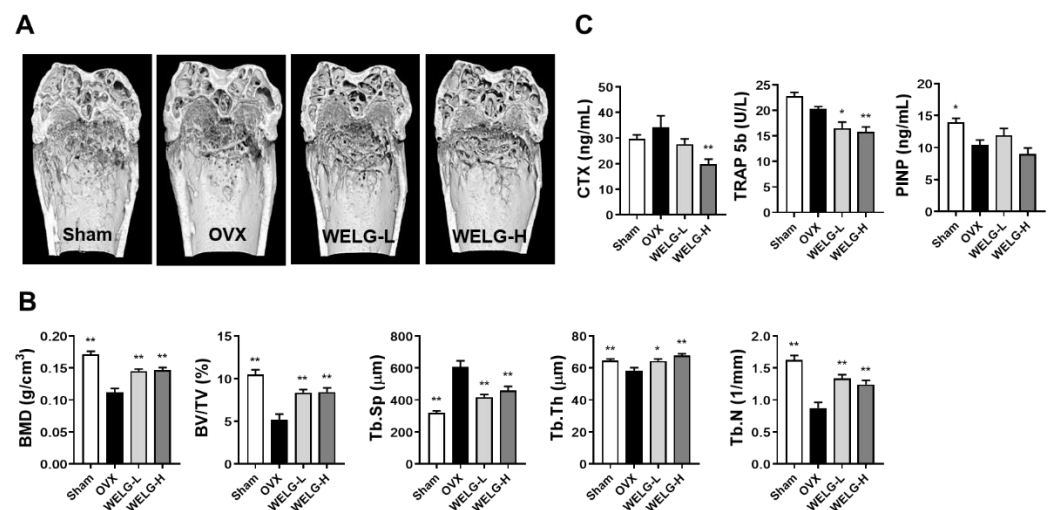


Figure 4. Preventive effects of WELG administration on OVX-induced bone loss in vivo. Mice were orally administered distilled water, WELG-L (100 mg/kg; Low), or WELG-H (300 mg/kg; High) for 6 weeks beginning 1 week after OVX or sham surgery. (A) Three-dimensional reconstruction images of the distal femur by micro-computed tomography. (B) Morphometric analyses of metaphyseal trabecular bone microstructure. (C) Serum levels of CTX, TRAP 5b and PINP. * $p < 0.05$, ** $p < 0.01$ versus OVX group.

Menopause triggers various physiological alterations due to the low transport ratio of estrogen to cholesterol [28,29]. Therefore, the levels of cholesterol in the blood, visceral fat, and body weight increase owing to the strong increase in fat tissues [28,29]. OVX mice showed an intense increase in body weight and gonadal fat weight, which was inhibited by WELG administration (Figure 5A). Osteoporosis is usually associated with increased bone marrow adipose tissue. During osteoporosis development, bone marrow mesenchymal stem cells show a high ability to differentiate into adipocytes rather than osteoblasts, which results in a decrease in bone formation and an increase in marrow fat deposition [30]. It has been shown that increased bone marrow fat inhibits bone healing and regeneration [31]. In this study, OVX significantly increased bone marrow fat accumulation, which was markedly inhibited by WELG administration (Figure 5B,C). Thus, our results suggest that WELG may have beneficial effects on bone by inhibiting both bone loss and bone marrow fat accumulation. In addition to bone marrow fat, WELG also inhibited OVX-induced fat accumulation in the liver (Figure 5B,C).

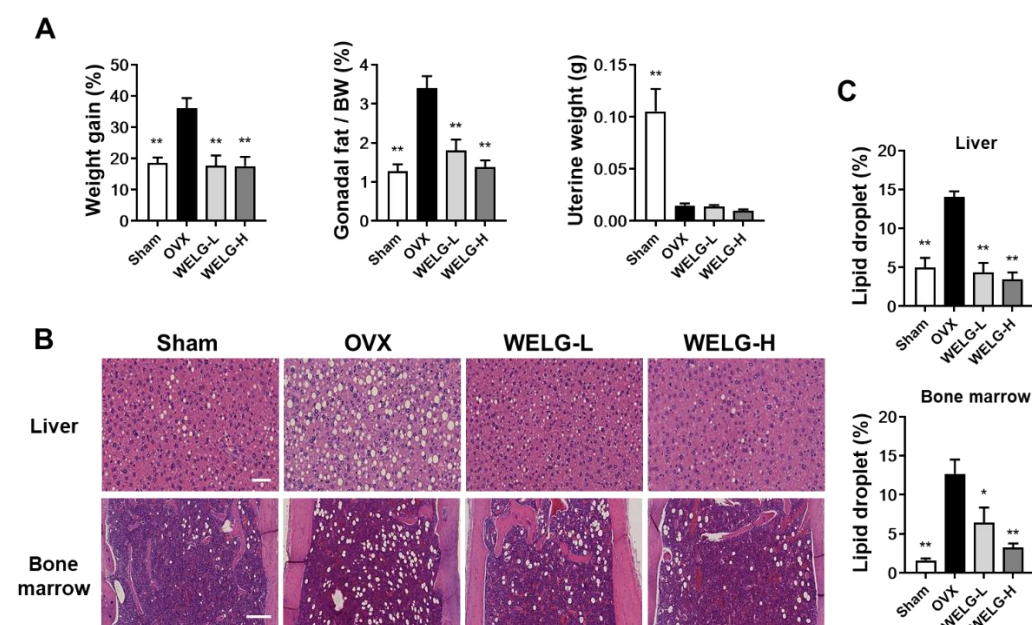


Figure 5. Inhibitory effect of WELG administration on OVX-induced fat accumulation. Mice were orally administered distilled water, WELG-L (100 mg/kg; Low), or WELG-H (300 mg/kg; High) for 6 weeks beginning 1 week after OVX or sham surgery. (A) Measurement of body weight changes for 7 weeks, gonadal fat weight/body weight (BW), and uterine weight. (B) Representative images of hematoxylin- and eosin-stained liver (scale bar, 50 μ m) and bone marrow (scale bar, 200 μ m) sections. (C) Quantification of lipid droplets in the liver and bone marrow sections. * $p < 0.05$, ** $p < 0.01$ versus OVX group.

In the OVX mice model, the weight of the uterus considerably decreases because removal of the ovary led to a decrease in the level of estrogen. In OVX mice, uterine weight significantly decreased compared with sham mice, which was not affected by WELG administration (Figure 5A). These results suggest that the beneficial effects WELG in OVX mice are independent of its potential estrogenic activity.

Our findings demonstrated that WELG has beneficial effects against bone loss, obesity, and ectopic fat deposition induced by OVX. These findings suggest that WELG can be a good candidate for simultaneously managing osteoporosis, obesity, and fat distribution in postmenopausal women.

2.4. Phytochemical Profiles of WELG

To determine the mechanism of the biological activity and phytochemical constituents of WELG, we investigated its phytochemical profile. The chemical compounds in WELG

were detected by ultrahigh-performance liquid chromatography–tandem mass spectrometry (UHPLC–MS/MS) and identified through its MS and MS/MS spectra, comparing with the previously reported MS spectra in a reference library [32,33]. Ultrahigh-performance liquid chromatography–tandem mass spectrometry (UHPLC–MS/MS) analysis of WELG identified four phenolics (5-O-caffeoylquinic acid, feruloylquinic acid, p-coumaric acid, and chlorogenic acid) and four flavonoids (apigenin-6-glucoside-8-xyloside, isoorientin, orientin, and isovitexin), as shown in Table 1. The ion chromatograms for the composition analysis of WELG are shown in Figure 6.

Table 1. The phytochemicals present in WELG as analyzed by UHPLC–MS/MS.

No	t_R (min)	[M – H] [−] (m/z)		Elemental Composition	Error (ppm)	MS/MS Fragments (m/z)	Identification
		Estimated	Calculated				
1	4.70	353.0878	353.0877	C ₁₆ H ₁₈ O ₉	2.808	191.0551, 179.0338, 135.0437	5-O-Caffeoylquinic acid *
2	5.25	353.0878	353.0876	C ₁₆ H ₁₈ O ₉	2.525	191.0550, 179.0338, 173.0443, 135.0436	Chlorogenic acid *
3	5.34	367.1050	367.1032	C ₁₇ H ₂₀ O ₉	2.292	193.0495, 173.0444, 149.0593, 134.0358	Feruloylquinic acid
4	5.93	563.1392	563.1399	C ₂₆ H ₂₈ O ₁₄	0.654	563.1392, 503.1185, 473.1083, 443.0967, 383.0767, 353.0669	Apigenin-6-glucoside-8-xyloside
5	5.97	447.0933	447.0930	C ₂₁ H ₂₀ O ₁₁	2.657	357.0612, 327.0507	Isoorientin *
6	6.33	447.0933	447.0930	C ₂₁ H ₂₀ O ₁₁	1.474	357.0613, 327.0508, 285.0398	Orientin *
7	6.47	163.0546	163.0387	C ₉ H ₈ O ₃	1.660	163.0388, 120.0520, 119.0486	p-Coumaric acid *
8	6.65	431.0989	431.0980	C ₂₁ H ₂₀ O ₁₀	1.686	341.0662, 311.0558	Isovitexin *

* compared with the retention time and MS spectral data of authentic standards.

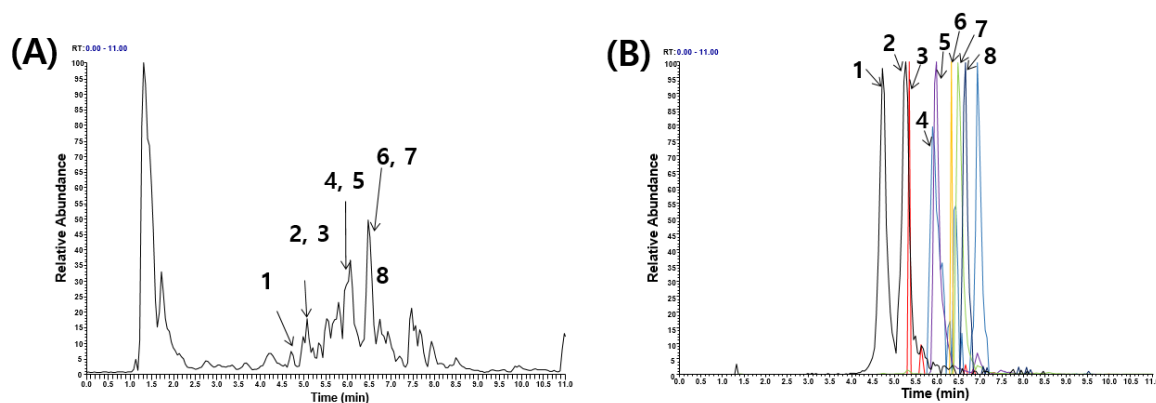


Figure 6. UHPLC–MS/MS analysis of WELG. (A) Base peak chromatogram in negative ion mode. (B) Extracted ion chromatogram of identified phytochemicals. 1, 5-O-caffeoylquinic acid; 2, chlorogenic acid; 3, feruloylquinic acid; 4, apigenin-6-glucoside-8-xyloside; 5, isoorientin; 6, orientin; 7, p-coumaric acid; 8, isovitexin.

Among these, four phytochemicals have been reported to exhibit potentially beneficial effects on bone. The two flavonoid glycosides, orientin (luteolin 8-C-glucoside) and isovitexin (apigenin-6-C-glucoside), have been shown to stimulate osteoblast differentiation in vitro [34,35]. The two phenolic compounds, p-coumaric acid and chlorogenic acid, have been reported to display a dual activity by inhibiting osteoclast differentiation and stimulating osteoblast differentiation in vitro, as well as to protecting against OVX-induced osteoporosis in vivo [36–39]. Therefore, it is likely that these active constituents of WELG cooperatively contribute to its anti-osteoclastic and anti-osteoporotic effects.

3. Materials and Methods

3.1. Materials

Alpha-modified minimum essential medium Eagle (α -MEM) was purchased from Hyclone (Logan, UT, USA). Fetal bovine and calf serums were purchased from Thermo Fisher Scientific (Waltham, MA, USA). AS-MX phosphate, fast red violet LB salt, naphthol, and VitD3 were obtained from Sigma-Aldrich (St. Louis, MO, USA). Lyophilized WELG was obtained from the National Development Institute of Korean Medicine (Gyeongsan, Korea). Briefly, dried leaves of *L. gracile* were extracted by heat reflux extraction with distilled water for 3 h, filtered, and lyophilized. The WELG powder was dissolved in distilled water prior to use.

3.2. Isolation and Generation of BMMs

Moue bone marrow was flushed from the femurs and tibias of C57BL/6J mice, and their red blood cells were lysed using ammonium-chloride-potassium buffer. These bone marrow cells were washed with PBS, passed through cell strainers, and then incubated in a complete medium, α -MEM supplemented with 10% FBS and 1% penicillin/streptomycin, supplemented with M-CSF (20 ng/mL) in tissue culture plate. After 24 h, nonadherent cells were cultured in a complete medium supplemented with MCSF (60 ng/mL) in non-coated plates. After five days, the adherent BMMs were dissociated, collected, and used for the osteoclast differentiation assay.

3.3. Cell Cytotoxicity Assay

BMMs were cultured for 1 day in the presence of M-CSF (60 ng/mL) with or without WELG (33.3, 100, and 200 μ g/mL). Cell cytotoxicity was measured using a CCK-8 reagent (Dojindo Molecular Technologies Inc., Rockville, MD, USA), and absorbance was measured at 450 nm using a microplate reader (Molecular Devices, San Jose, CA, USA).

3.4. Osteoclast Differentiation Assay

To examine the effect of WELG on osteoclast differentiation in a BMM–osteocyte co-culture system, MLO-Y4 cells (Kerafast, Boston, MA, USA) cultured for 12 h were co-cultured with BMMs for 5 days with or without WELG (33.3, 100, and 200 μ g/mL) in the presence of VitD3 (10 nM). To assess a direct inhibitory effect of WELG on osteoclast differentiation, BMMs were cultured with or without WELG for 4 days in the presence of M-CSF (60 ng/mL) and RANKL (50 ng/mL).

3.5. TRAP Staining

Cells were fixed with 10% formalin, permeabilized with 0.1% Triton X-100 in PBS, and then stained with TRAP staining buffer (50 mM sodium tartrate, 0.12 M sodium acetate, naphthol AS-MX phosphate, and fast red violet LB salt, pH 5.2). TRAP-stained cells were washed with distilled water and photographed.

3.6. Western Blot Assay

BMMs were harvested and lysed using lysis buffer (iNtRON Biotechnology, Seongnam, Korea). The supernatants were collected as total cell lysates. Protein concentration was quantified using a BCA protein assay kit (Thermo Fisher Scientific, Waltham, MA, USA). Proteins were separated by SDS-PAGE and transferred onto polyvinylidene difluoride (PVDF) membranes. After blocking with 5% skim milk, membranes were incubated with specific primary antibodies (1:1000 dilution) at 4 °C. The primary antibodies are as follows: Phospho-JNK, JNK, phospho-p38, p38, phospho-I κ B α , I κ B α , and β -actin obtained from Cell Signaling Technology (Danvers, MA, USA); NFATc1 and c-Fos obtained from Santa Cruz Biotechnology, Inc. (Dallas, TX, USA). The membranes were then detected using the corresponding HRP-conjugated secondary antibodies (1:5000 dilution) at room temperature. Finally, chemiluminescent signals were analyzed using a ChemiDoc Imaging System (Bio-Rad, Hercules, CA, USA).

3.7. Quantitative Real-Time Polymerase Chain Reaction

Total RNA was isolated using an RNA-spin™ Total RNA Extraction Kit (iNtRON Biotechnology, Seongnam, Korea). cDNA was synthesized from total RNA using a High-Capacity cDNA Reverse Transcription Kit (Thermo Fisher Scientific). The generated cDNA was amplified with TaqMan Universal Master Mix II (Applied Biosystems, Foster City, CA, USA) and TaqMan probes for the target genes *Tnfsf11* (Mm00441908_m1), *Tnfrsf11b* (Mm0043542_m1), *c-Fos* (Mm00487425_m1), *Nfatc1* (Mm00479445_m1), *Prdm1* (Mm00476128_m1), *Ifnb1* (Mm00439552_s1), *Irf8* (Mm00492567_m1), *MafB* (Mm00627481_s1), *Ctsk* (Mm00484036_m1), *Itgb3* (Mm00443980_m1), *Mmp9* (Mm00442991_m1), and 18S rRNA (Hs99999901_s1) using an ABI 7500 Real-Time PCR Instrument (Applied Biosystems).

3.8. Animal Study

Seven-week-old C57BL/6J female specific-pathogen-free mice were housed with free access to a standard rodent chow diet and water. Mice were anesthetized with zoletil and rompun, subjected to sham or OVX surgery, and then divided into four groups of six mice each ($n = 6/\text{group}$): sham, OVX, and OVX with low-dose WELG (WELG-L, 100 mg/kg/day) and high-dose WELG (WELG-H, 300 mg/kg/day). One week after OVX surgery, mice were fed a purified low-fat diet (D12450B, Research Diet, New Brunswick, NJ, USA) and orally administered either distilled water, WELG-L, or WELG-H for six weeks. Serum was obtained after sacrifice, and serum levels of CTX, TRAP 5b and PINP were measured using specific ELISA kits (Immunodiagnostic Systems Ltd., London, UK).

For femoral trabecular bone analysis, the distal end of the right femur was scanned using the SkyScan 1276 micro-computed tomography system (Bruker, Kontich, Belgium). The scanned images were reconstructed and analyzed using SkyScan software (Bruker, Kontich, Belgium).

For histological staining, the liver and femur were fixed, dehydrated, embedded into a paraffin block, sectioned into a 5 μm thick slices, and stained with hematoxylin and eosin. The femur was decalcified with RDO Gold (RDO, Aurora, IL, USA) for 1 week prior to dehydration. The stained tissue sections were photographed, and lipid droplet areas were measured using the Image J software.

3.9. UHPLC–MS/MS Analysis for Phytochemical Profiles

The WELG was analyzed using a Thermo Dionex UltiMate 3000 HPLC system equipped with a Thermo Q-Exactive mass spectrometer (Thermo Fisher Scientific). An Acquity BEH C18 column (1.7 μm , 100 mm \times 2.1 mm) was used for chromatographic separation. The operating protocol was based on a previous study with minor modifications [40,41]. Upon injection of 3- μL samples, they were chromatographically separated using a binary gradient consisting of 0.1% formic acid in water and acetonitrile. The reference standards, orientin, isovitexin, isoorientin, 5-O-caffeoylquinic acid, chlorogenic acid, and p-coumaric acid were obtained from Targetmol (Wellesley Hills, MA, USA).

3.10. Statistical Analysis

Data are presented as mean \pm standard deviation (SD) for in vitro experiments and as mean \pm standard error of the mean (SEM) in animal experiments. The values were assessed by one-way analysis of variance (ANOVA) followed by Dunnett's test or two-way ANOVA followed by Sidak's test, and values of $p < 0.05$ were regarded as statistically significant.

4. Conclusions

In summary, this study demonstrated that WELG can inhibit osteoclast differentiation and have a protective effect on OVX-induced bone loss. WELG directly inhibited the differentiation of osteoclast precursors into osteoclasts by suppressing RANKL-induced activation of MAPKs and NF- κ B, upregulation of positive regulators, and downregulation of negative regulators of osteoclastogenesis. In an OVX-induced postmenopausal osteoporosis mouse model, WELG administration prevented bone loss, weight gain, and ectopic

fat accumulation without affecting uterine atrophy. Furthermore, we identified active constituents which have bone-protective effects in WELG. Taken together, our findings suggest that WELG might be a potential candidate for the simultaneous management of osteoporosis and obesity in postmenopausal women.

Author Contributions: Conceptualization, H.H.; methodology, S.-A.J., S.-J.L., S.C.K., J.A.R. and H.H.; validation and formal analysis, S.-A.J., S.-J.L., S.C.K. and J.A.R.; writing—original draft preparation, S.-A.J., S.-J.L. and H.H.; writing—review and editing, S.-J.L. and H.H.; project administration, H.H.; funding acquisition, H.H. All authors have read and agreed to the published version of the manuscript.

Funding: This study was supported by the Korea Institute of Oriental Medicine, Ministry of Science and ICT, Republic of Korea [grant number: KSN2021330].

Institutional Review Board Statement: The study was conducted in accordance with the Declaration of Helsinki, and approved by the Institutional Animal Care and Use Committee (IACUC) at Knotus (Guri, Korea) (approval number: 19-KE-216).

Informed Consent Statement: Not applicable.

Data Availability Statement: All data of this study are provided within this study.

Conflicts of Interest: The authors declare no conflict of interest.

References

1. Kim, J.M.; Lin, C.; Stavre, Z.; Greenblatt, M.B.; Shim, J.H. Osteoblast-Osteoclast Communication and Bone Homeostasis. *Cells* **2020**, *9*, 73. [[CrossRef](#)] [[PubMed](#)]
2. Wada, T.; Nakashima, T.; Hiroshi, N.; Penninger, J.M. RANKL-RANK signaling in osteoclastogenesis and bone disease. *Trends Mol. Med.* **2006**, *12*, 17–25. [[CrossRef](#)]
3. Gao, Y.; Patil, S.; Jia, J. The Development of Molecular Biology of Osteoporosis. *Int. J. Mol. Sci.* **2021**, *22*, 8182. [[CrossRef](#)] [[PubMed](#)]
4. McNamara, L.M. Perspective on post-menopausal osteoporosis: Establishing an interdisciplinary understanding of the sequence of events from the molecular level to whole bone fractures. *J. R. Soc. Interface* **2010**, *7*, 353–372. [[CrossRef](#)] [[PubMed](#)]
5. Kim, J.H.; Kim, N. Signaling Pathways in Osteoclast Differentiation. *Chonnam. Med. J.* **2016**, *52*, 12–17. [[CrossRef](#)] [[PubMed](#)]
6. Park, J.H.; Lee, N.K.; Lee, S.Y. Current Understanding of RANK Signaling in Osteoclast Differentiation and Maturation. *Mol. Cells* **2017**, *40*, 706–713. [[CrossRef](#)] [[PubMed](#)]
7. Wong, B.R.; Josien, R.; Lee, S.Y.; Vologodskaya, M.; Steinman, R.M.; Choi, Y. The TRAF family of signal transducers mediates NF-kappaB activation by the TRANCE receptor. *J. Biol. Chem.* **1998**, *273*, 28355–28359. [[CrossRef](#)] [[PubMed](#)]
8. Gohda, J.; Akiyama, T.; Koga, T.; Takayanagi, H.; Tanaka, S.; Inoue, J. RANK-mediated amplification of TRAF6 signaling leads to NFATc1 induction during osteoclastogenesis. *EMBO J.* **2005**, *24*, 790–799. [[CrossRef](#)]
9. Huang, H.; Chang, E.J.; Ryu, J.; Lee, Z.H.; Lee, Y.; Kim, H.H. Induction of c-Fos and NFATc1 during RANKL-stimulated osteoclast differentiation is mediated by the p38 signaling pathway. *Biochem. Biophys. Res. Commun.* **2006**, *351*, 99–105. [[CrossRef](#)]
10. Ikeda, F.; Nishimura, R.; Matsubara, T.; Tanaka, S.; Inoue, J.; Reddy, S.V.; Hata, K.; Yamashita, K.; Hiraga, T.; Watanabe, T.; et al. Critical roles of c-Jun signaling in regulation of NFAT family and RANKL-regulated osteoclast differentiation. *J. Clin. Investig.* **2004**, *114*, 475–484. [[CrossRef](#)]
11. Yamashita, T.; Yao, Z.; Li, F.; Zhang, Q.; Badell, I.R.; Schwarz, E.M.; Takeshita, S.; Wagner, E.F.; Noda, M.; Matsuo, K.; et al. NF-kappaB p50 and p52 regulate receptor activator of NF-kappaB ligand (RANKL) and tumor necrosis factor-induced osteoclast precursor differentiation by activating c-Fos and NFATc1. *J. Biol. Chem.* **2007**, *282*, 18245–18253. [[CrossRef](#)] [[PubMed](#)]
12. Takayanagi, H.; Kim, S.; Koga, T.; Nishina, H.; Isshiki, M.; Yoshida, H.; Saiura, A.; Isobe, M.; Yokochi, T.; Inoue, J.; et al. Induction and activation of the transcription factor NFATc1 (NFAT2) integrate RANKL signaling in terminal differentiation of osteoclasts. *Dev. Cell* **2002**, *3*, 889–901. [[CrossRef](#)]
13. Aliprantis, A.O.; Ueki, Y.; Sulyanto, R.; Park, A.; Sigrist, K.S.; Sharma, S.M.; Ostrowski, M.C.; Olsen, B.R.; Glimcher, L.H. NFATc1 in mice represses osteoprotegerin during osteoclastogenesis and dissociates systemic osteopenia from inflammation in cherubism. *J. Clin. Investig.* **2008**, *118*, 3775–3789. [[CrossRef](#)] [[PubMed](#)]
14. Tanaka, S.; Nakamura, K.; Takahashi, N.; Suda, T. Role of RANKL in physiological and pathological bone resorption and therapeutics targeting the RANKL-RANK signaling system. *Immunol. Rev.* **2005**, *208*, 30–49. [[CrossRef](#)] [[PubMed](#)]
15. Kim, A.; Im, M.; Gu, M.J.; Ma, J.Y. Ethanol extract of Lophatheri Herba exhibits anti-cancer activity in human cancer cells by suppression of metastatic and angiogenic potential. *Sci. Rep.* **2016**, *6*, 36277. [[CrossRef](#)]
16. Lai, K.H.; Chen, P.J.; Chen, C.C.; Yang, S.H.; El-Shazly, M.; Chang, Y.C.; Wu, Y.H.; Wu, Y.H.; Wang, Y.H.; Hsieh, H.L.; et al. Lophatherum gracile Brongn. attenuates neutrophilic inflammation through inhibition of JNK and calcium. *J. Ethnopharm.* **2021**, *264*, 113224. [[CrossRef](#)]

17. Rozema, E.; Atanasov, A.G.; Fakhrudin, N.; Singhuber, J.; Namduang, U.; Heiss, E.H.; Reznicek, G.; Huck, C.W.; Bonn, G.K.; Dirsch, V.M.; et al. Selected Extracts of Chinese Herbal Medicines: Their Effect on NF- κ B, PPAR α and PPAR γ and the Respective Bioactive Compounds. *Evid. Based Complement. Altern. Med.* **2012**, *2012*, 983023. [[CrossRef](#)]
18. Wang, Y.; Chen, M.; Zhang, J.; Zhang, X.L.; Huang, X.J.; Wu, X.; Zhang, Q.W.; Li, Y.L.; Ye, W.C. Flavone C-glycosides from the leaves of *Lophatherum gracile* and their in vitro antiviral activity. *Planta Med.* **2012**, *78*, 46–51. [[CrossRef](#)]
19. He, Q.; Li, Y.; Liu, J.; Zhang, P.; Yan, S.; He, X.; Zhang, A. Hepatoprotective Activity of *Lophatherum gracile* Leaves of Ethanol Extracts Against Carbon Tetrachloride-induced Liver Damage in Mice. *Int. J. Pharmacol.* **2016**, *12*, 387–393. [[CrossRef](#)]
20. Nakashima, T.; Hayashi, M.; Fukunaga, T.; Kurata, K.; Oh-Hora, M.; Feng, J.Q.; Bonewald, L.F.; Kodama, T.; Wutz, A.; Wagner, E.F.; et al. Evidence for osteocyte regulation of bone homeostasis through RANKL expression. *Nat. Med.* **2011**, *17*, 1231–1234. [[CrossRef](#)]
21. Xiong, J.; Piemontese, M.; Onal, M.; Campbell, J.; Goellner, J.J.; Dusevich, V.; Bonewald, L.; Manolagas, S.C.; O'Brien, C.A. Osteocytes, not Osteoblasts or Lining Cells, are the Main Source of the RANKL Required for Osteoclast Formation in Remodeling Bone. *PLoS ONE* **2015**, *10*, e0138189. [[CrossRef](#)] [[PubMed](#)]
22. Zhao, S.; Zhang, Y.K.; Harris, S.; Ahuja, S.S.; Bonewald, L.F. MLO-Y4 osteocyte-like cells support osteoclast formation and activation. *J. Bone Min. Res.* **2002**, *17*, 2068–2079. [[CrossRef](#)] [[PubMed](#)]
23. Matsuo, K.; Galson, D.L.; Zhao, C.; Peng, L.; Laplace, C.; Wang, K.Z.; Bachler, M.A.; Amano, H.; Aburatani, H.; Ishikawa, H.; et al. Nuclear factor of activated T-cells (NFAT) rescues osteoclastogenesis in precursors lacking c-Fos. *J. Biol. Chem.* **2004**, *279*, 26475–26480. [[CrossRef](#)] [[PubMed](#)]
24. Kim, K.; Kim, J.H.; Lee, J.; Jin, H.M.; Kook, H.; Kim, K.K.; Lee, S.Y.; Kim, N. MafB negatively regulates RANKL-mediated osteoclast differentiation. *Blood* **2007**, *109*, 3253–3259. [[CrossRef](#)] [[PubMed](#)]
25. Zhao, B.; Takami, M.; Yamada, A.; Wang, X.; Koga, T.; Hu, X.; Tamura, T.; Ozato, K.; Choi, Y.; Ivashkiv, L.B.; et al. Interferon regulatory factor-8 regulates bone metabolism by suppressing osteoclastogenesis. *Nat. Med.* **2009**, *15*, 1066–1071. [[CrossRef](#)]
26. Nishikawa, K.; Nakashima, T.; Hayashi, M.; Fukunaga, T.; Kato, S.; Kodama, T.; Takahashi, S.; Calame, K.; Takayanagi, H. Blimp1-mediated repression of negative regulators is required for osteoclast differentiation. *Proc. Natl. Acad. Sci. USA* **2010**, *107*, 3117–3122. [[CrossRef](#)]
27. Takayanagi, H.; Kim, S.; Matsuo, K.; Suzuki, H.; Suzuki, T.; Sato, K.; Yokochi, T.; Oda, H.; Nakamura, K.; Ida, N.; et al. RANKL maintains bone homeostasis through c-Fos-dependent induction of interferon-beta. *Nature* **2002**, *416*, 744–749. [[CrossRef](#)]
28. Li, H.; Sun, R.; Chen, Q.; Guo, Q.; Wang, J.; Lu, L.; Zhang, Y. Association between HDL-C levels and menopause: A meta-analysis. *Hormones* **2021**, *20*, 49–59. [[CrossRef](#)]
29. Davis, S.R.; Castelo-Branco, C.; Chedraui, P.; Lumsden, M.A.; Nappi, R.E.; Shah, D.; Villaseca, P.; Writing Group of the International Menopause Society for World Menopause, D. Understanding weight gain at menopause. *Climacteric* **2012**, *15*, 419–429. [[CrossRef](#)]
30. Muruganandan, S.; Govindarajan, R.; Sinal, C.J. Bone Marrow Adipose Tissue and Skeletal Health. *Curr. Osteoporos. Rep.* **2018**, *16*, 434–442. [[CrossRef](#)]
31. Ambrosi, T.H.; Scialdone, A.; Graja, A.; Gohlke, S.; Jank, A.M.; Bocian, C.; Woelk, L.; Fan, H.; Logan, D.W.; Schurmann, A.; et al. Adipocyte Accumulation in the Bone Marrow during Obesity and Aging Impairs Stem Cell-Based Hematopoietic and Bone Regeneration. *Cell Stem Cell* **2017**, *20*, 771–784 e776. [[CrossRef](#)] [[PubMed](#)]
32. Fu, Q.; Wang, H.; Lan, Y.; Li, S.; Hashi, Y.; Chen, S. High-throughput and sensitive screening of compounds with deoxyribonucleic acid-binding activity by a high-performance liquid chromatography-tandem mass spectrometry-fluorescence detection technique using palmitate as a fluorescence probe. *J. Chromatogr. A* **2014**, *1323*, 123–134. [[CrossRef](#)] [[PubMed](#)]
33. Liu, X.; Wang, Y.; Ge, W.; Cai, G.; Guo, Y.; Gong, J. Spectrum-effect relationship between ultra-high-performance liquid chromatography fingerprints and antioxidant activities of *Lophatherum gracile* Brongn. *Food Sci. Nutr.* **2022**, *10*, 1592–1601. [[CrossRef](#)] [[PubMed](#)]
34. Nash, L.A.; Sullivan, P.J.; Peters, S.J.; Ward, W.E. Rooibos flavonoids, orientin and luteolin, stimulate mineralization in human osteoblasts through the Wnt pathway. *Mol. Nutr. Food Res.* **2015**, *59*, 443–453. [[CrossRef](#)] [[PubMed](#)]
35. Pal, S.; Singh, M.; Porwal, K.; Rajak, S.; Das, N.; Rajput, S.; Trivedi, A.K.; Maurya, R.; Sinha, R.A.; Siddiqi, M.I.; et al. Adiponectin receptors by increasing mitochondrial biogenesis and respiration promote osteoblast differentiation: Discovery of isovitexin as a new class of small molecule adiponectin receptor modulator with potential osteoanabolic function. *Eur. J. Pharm.* **2021**, *913*, 174634. [[CrossRef](#)]
36. Kwak, S.C.; Lee, C.; Kim, J.Y.; Oh, H.M.; So, H.S.; Lee, M.S.; Rho, M.C.; Oh, J. Chlorogenic acid inhibits osteoclast differentiation and bone resorption by down-regulation of receptor activator of nuclear factor kappa-B ligand-induced nuclear factor of activated T cells c1 expression. *Biol. Pharm. Bull.* **2013**, *36*, 1779–1786. [[CrossRef](#)]
37. Yamaguchi, M.; Lai, Y.L.; Uchiyama, S.; Nakagawa, T. Oral administration of phytochemical p-hydroxycinnamic acid prevents bone loss in ovariectomized rats. *Mol. Cell. Biochem.* **2008**, *311*, 31–36. [[CrossRef](#)]
38. Yamaguchi, M.; Weitzmann, M.N. The bone anabolic carotenoid p-hydroxycinnamic acid promotes osteoblast mineralization and suppresses osteoclast differentiation by antagonizing NF- κ B activation. *Int. J. Mol. Med.* **2012**, *30*, 708–712. [[CrossRef](#)]
39. Zhou, R.P.; Lin, S.J.; Wan, W.B.; Zuo, H.L.; Yao, F.F.; Ruan, H.B.; Xu, J.; Song, W.; Zhou, Y.C.; Wen, S.Y.; et al. Chlorogenic Acid Prevents Osteoporosis by Shp2/PI3K/Akt Pathway in Ovariectomized Rats. *PLoS ONE* **2016**, *11*, e0166751. [[CrossRef](#)]

40. Zhang, C.; Ren, B.; Lin, Z.; Tong, L.; Wang, H.; Chen, S. An analysis method for simultaneous screening of deoxyribonucleic acid-binding active compounds and investigating their mechanisms by ultra-fast liquid chromatography tandem mass spectrometry coupled with fluorescence detection technology. *J. Chromatogr. A* **2015**, *1381*, 160–172. [[CrossRef](#)]
41. Hwang, Y.H.; Jang, S.A.; Kim, T.; Ha, H. Forsythia suspensa Protects against Bone Loss in Ovariectomized Mice. *Nutrients* **2019**, *11*, 1831. [[CrossRef](#)] [[PubMed](#)]